CHARACTERIZATION OF THE ALUMINA LAYER DEPOSITED BY PLASMA SPRAY DEPOSITION ON THE HARDOX STEEL FOR BALLISTIC PROTECTION

Cosmin NICOLESCU[1*], Corneliu MUNTEANU[2,3], Ștefan-Constantin LUPESCU[4], Viorel ȚIGĂNESCU [5], Marian MICULESCU[6], Bogdan ISTRATE[7], Iulian-Vasile ANTONIAC[2,8]

This research aimed to improve the mechanical properties of HARDOX 450 steel and increase its ballistic properties. In this paper, Al2O3 ceramic coatings were deposited on HARDOX 450 steel using the Atmospheric Plasma Spraying (APS) method. The deposition process was performed on 5 plates on both sides, and the deposition layer was approximately 200 microns. Optical and scanning electron microscopy and XRD analysis were performed for microstructural and morphological characterization of coated and uncoated HARDOX 450 steels. The adhesion was assessed through a scratch test.

Keywords: Armor steel, Al_2O_3 coating, APS method, microstructure.

1. Introduction

Protective materials are required worldwide for various purposes to keep personnel and equipment safe and secure. From the material used point of view, better properties are needed for the anti-blast and anti-penetration capacity of metallic thin-walled structures, such as equipment, buildings, and military vehicles, which are widespread in most parts of the modern world [1].

[1*] PhD student, Faculty of Materials Science and Engineering, National University of Science and Technology POLITEHNICA Bucharest, corresponding author, e-mail: nicolescu_cosmin@yahoo.com,
[2] Prof., Academy of Romanian Scientista, Bucharest, Romania
[3] Prof., Faculty of Mechanical Engineering, "Gheorghe Asachi" Technical University of Iasi, Romania, e-mail: corneliu.munteanu@academic.tuiasi.ro
[4] Lect., Faculty of Mechanical Engineering, Mechatronics and Management, "Ștefan cel Mare" University of Suceava, Romania, e-mail: lupescustefan@ymail.com
[5] Prof., Technical Science Academy Romania, Bucharest, Romania, e-mail: viorel.tiganescu@mta.ro
[6] Prof., Faculty of Materials Science and Engineering, National University of Science and Technology POLITEHNICA Bucharest, e-mail: marian.miculescu@upb.ro
[7] Lect., Faculty of Mechanical Engineering, "Gheorghe Asachi" Technical University of Iasi, Romania, e-mail: bogdan.istrate@academic.tuiasi.ro
[8] Prof., Faculty of Materials Science and Engineering, National University of Science and Technology POLITEHNICA Bucharest, e-mail: antoniac.iulian@gmail.com

Although many materials, such as ceramics, polymers, and composites, have suitable properties for protection purposes, steel remains the most used material for protective structures.

Compared to other materials, steels have the overall properties required for protective structures, such as high strength and hardness, high ductility, high formability, and reasonable cost. However, high-quality armor steels are still expensive, and efforts are being made to reduce the costs attached to these types of steels or to develop new and less expensive steels with protective properties [2–4].

High-strength steel is often used as a protective element in transportation, military industry, and mining. This steel is used in many industries to make armor, containers, bunkers, dump truck bodies, and other mechanical parts. These must have excellent mechanical properties such as high strength and stiffness, high welding performance, high impact and wear resistance, fatigue resistance, good ductility, machinability, and cold forming [5–7]. HARDOX steel fully meets these requirements and is characterized by high strength even when used in harsh conditions and exhibits very high impact resistance at both high and low temperatures [8,9]. It is meaningful to notice that boriding (adding a layer of boride) of HARDOX 450 steel considerably increases its protective properties under the influence of X-rays and gamma rays, making it very suitable for producing protective gloves for the military industry [10].

Another class of materials used as protective materials is ceramics due to their very high hardness and compressive strength, which are associated with a low specific weight due to their low density. Commonly used ceramic materials include alumina (Al_2O_3), boron carbide (B_4C), silicon nitride (S_3N_4), silicon carbide (SiC), and titanium diboride (TiB_2). The ballistic properties, availability, production technology, and workability determine where they are used. The most affordable and widely used ceramic is alumina. Unfortunately, ceramic materials are also very brittle and may easily crack because of the tension waves developed when they are subjected to impacts [11,12].

The shape and size of the ceramic elements significantly impact the armor's ballistic resistance. According to Su and Chen [13] ballistic simulation tests show differences between ceramic panels' traditional hexagonal and square shapes. Studies have shown that hexagonal blocks perform better at panel intersections, while the ballistic performance of square blocks and regular hexagonal units is essentially the same in the panel's central and eccentric regions.

Metals and ceramics differ in the mechanisms by which they absorb projectile kinetic energy. Due to the interaction of various stress factors during impact and the short time associated with crack initiation and propagation, no single property correlates with ballistic performance [14–16].

It should be noted that, in addition to HARDOX Extreme, HARDOX 450 steel stands out among other steels offered by steel manufacturers with similar

properties to HARDOX steel [17]. It is characterized by an average hardness - depending on the sheet thickness - even higher than 600 units on the Brinell hardness tester and a very high static strength value - Rm ≥ 2000 MPa. Therefore, a reasonable premise justifies the possibility of using the high strength index of HARDOX 450 steel for equipment and selected machine components, the structural elements of which are connected by welding techniques [18,19].

In general, the blast and impact resistance of metallic structures can be enhanced by growing the substrate's thickness or by using innovative composite materials [3,4,20]. Anyway, such methods will significantly increase the weight and volume of the structure, which can have a negative impact on the functionality of the structure itself. Furthermore, because of the limitations of the hardness and tensile strength of the material itself, the method mentioned above cannot achieve the best results [21].

Recently, the metal protective industry has focused research on improving the performance of matrix materials using a thin film, surface modification, and coating techniques. In particular, the thermal spraying technology of ceramic coatings plays an essential role in improving the blast resistance and penetration resistance of materials [20,22].

Many industries use different types of thermal spraying in many critical applications. Thermal spraying is an industrial method of obtaining surfaces with unique properties [23,24]. Dorfman M. [23] describes the function of the layers deposited in various applications, among which we can refer to the repair of surfaces, the improvement of behavior to abrasive wear, protection against corrosion, erosion, and adhesive wear. The most used thermal spraying processes available are High-Velocity oxy-fuel spraying (HVOF), Plasma Spraying (PS), Combustion Flame Spraying (CFS), Vacuum Plasma Spraying (VPS), and Two-Wire Electric Arc Spraying (TWEAS). Atmospheric Plasma Spraying (APS) is widely used to develop ceramic, oxide, or non-oxide coatings due to its higher deposition rate and lower cost [25,26]. Currently, for industrial applications, the use of atmospheric plasma spray with robotic arms increases the possibility of enhancing the properties of steel, such as erosion, resistance to corrosion, and wear of different grades of ceramic coatings. In addition to the high deposition rate of the process, it also addresses various quality issues characteristic of APS layers, including high porosity, poor adhesion, and reduced gas jet velocity conducting to ceramic layers with poor mechanical properties, poor wear resistance, and reduced high-temperature corrosion resistance [27].

Plasma deposition has advantages such as more significant surface areas covered, higher deposition rates, and deposition possibilities for a wide range of materials (metals, ceramics, or polymers). For its application in industry, the parameters for optimal deposition must be determined. This directly depends on the

type of deposited layers and substrate, including the number of layers deposited, spray distance, and substrate roughness [28].

This article describes the deposition method: plasma jet spraying and presents the experimental results obtained on HARDOX 450 steel samples coated with alumina, from the point of view of the material's structure, chemical composition, adhesion and mechanical properties. Different materials are used as raw materials for Atmospheric Plasma Spraying (APS), but the most frequently used one is alumina (Al_2O_3). For this method, alumina powders with sintered and agglomerated morphology are used. When speaking about increasing the wear resistance and improving the corrosion resistance against chemical agents, coatings similar to protective solutions that have a pure alumina composition were used [29–32]. For this reason, the authors decided to carry out scratch tests for surface analysis, optical and SEM microscopy tests, and XRD analyses on both the base material and the material with plasma jet deposition. These coatings provide functional surfaces that protect or modify the substrate's behavior.

2. Materials and methods

The work aims to find optimal variants of thermal or cold deposition in order to obtain the highest possible hardness and wear resistance for armor in military equipment.

The purpose of testing plates obtained by plasma deposition techniques is to obtain data necessary for a preliminary evaluation of their properties. In this sense, the conditions that must be met by the plates deposited with ceramic powder must be as close as possible to their conditions of use. Therefore, the similarity between the methods of testing and developing the coatings becomes necessary to evaluate the success as accurately as possible. Another essential requirement for a good preliminary test is to ensure the repeatability of the data and its validity to predict the maximum performance of the coating. To correctly select the powder deposited on the base material, it was subjected to spectroscopy tests using the Hitachi Foundry-Master spectrometer. Three tests were performed in three different areas; the results are shown in Table 1.

Table 1

Spectroscopy test results

	Fe [%]	C [%]	Si [%]	Mn [%]	P [%]	S [%]	Cr [%]
1	79.1	3.15	>7.00	1.50	0.0679	0.172	0.189
2	81.1	1.73	>7.00	1.35	0.0440	0.124	0.185
3	81.1	1.92	>7.00	1.41	0.0575	0.129	0.199
Ø	80.4	2.27	>7.00	1.42	0.0565	0.141	0.191
RSD	1.40	34.80	0.00	5.55	21.18	18.95	3.81
	Mo [%]	Ni [%]	Al [%]	Co [%]	Cu [%]	Nb [%]	Ti [%]

1	0.153	7.51	>0.150	0.0232	0.128	0.167	0.116
2	0.151	7.29	>0.150	0.0240	0.113	0.144	0.1000
3	0.148	7.04	>0.150	0.0122	0.107	0.124	0.0991
Ø	0.151	7.28	>0.150	0.0198	0.116	0.145	0.105
RSD	1.77	3.20	0.00	33.17	9.33	14.79	9.18
	V [%]	W [%]	Sn [%]				
1	0.0723	>0.400	0.0806				
2	0.0674	>0.400	0.0703				
3	0.0585	>0.400	0.0684				
Ø	0.0661	>0.400	0.0731				
RSD	10.60	0.00	9.00				

The chosen powder was an oxide of Al (Al_2O_3), Metco 105NS (datasheet: DSM-0237.3_Al_2O_3), to highlight the material`s hardness and wear resistance. Alumina was deposited using the SPRAYWIZARD 9MCE plasma jet deposition installation, like is shown Fig. 1. The samples to be deposited were sandblasted to remove any layer of oxides or grease on their surface. The deposition process was performed on 5 plates on both sides, and as Table 1 shows, the deposition layer is approximately 200 microns.

After deposition, the plates underwent a heat treatment with the help of the oven for Nabertherm thermal treatments, which consisted of raising temperatures to 250 degrees Celsius with a 30-minute hold and a slow cooling inside the oven. After cooling, the plates were debited to be analyzed structurally and tribologically.

The samples taken after cutting were polished with abrasive paper of different grits from 150 to 1800 SiC to obtain a uniform surface. The surface of each sample was polished to a final finish with an alumina suspension of 0.05 µm. Samples were etched using 4% w/w nitric acid as standard for 5–8 seconds, washed thoroughly with water and alcohol, then dried with hot air.

The optical microscope Leica 5000 DMI was used to highlight the microstructures. The surface and interface were investigated by scanning electron microscopy, using an SEM Quanta 200 3D equipped with an EDX detector. For the structural analysis, an X'Pert PRO MRD X-ray diffractometer was used. The parameters of the micro-scaling analysis are as follows: a constant load of 5 N at a distance of 4 mm for a single determination. Using a metal indenter, we also performed determinations with a constant load of 5 N for the indentation test.

Fig. 1. The deposited tiles and the arm of the deposition installation

3. Results and discussions

3.1. Optical microscopy results

The optical micrographs for both samples, the base HARDOX steel and the HARDOX steel coated with Al_2O_3, are presented in Fig. 2, respectively in Fig. 3, at different magnification scales.

The coating layer is relatively homogeneous on the entire surface of the samples. Instead, on the base material, we can observe a sorbic structure that appeared as an effect of the heat treatment, which consisted of raising temperatures to 250 degrees Celsius with a 30-minute hold and a slow cooling inside the oven.

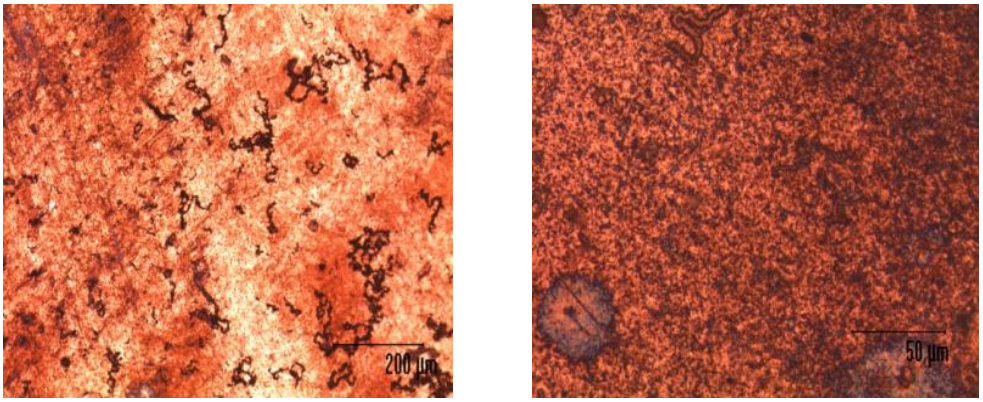

(a) (b)

Fig. 2. Optical microscopy images for HARDOX steel: a) 100X, b) 1000X

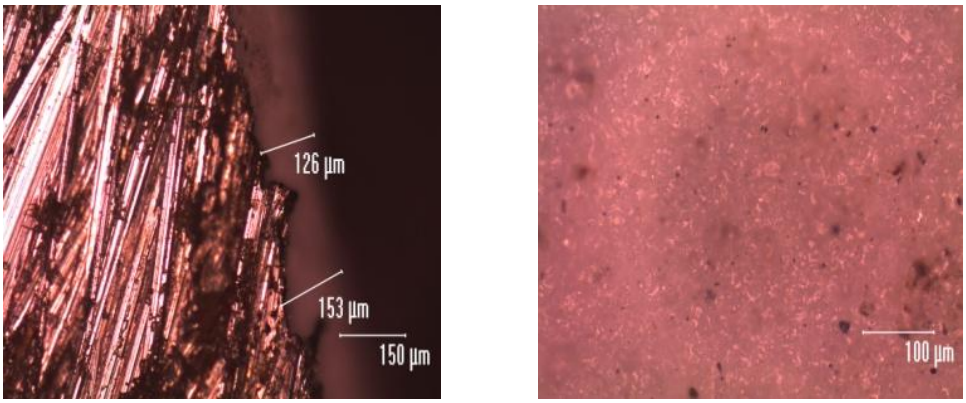

(a) (b)

Fig. 3. Optical microscopy images for alumina coatings on HARDOX steel: a) 100X, b) 200X

3.2. Scanning electron microscopy results.

The morphological aspects of the experimental samples revealed by scanning electron microscopy are presented in more detail in Fig. 4 (a, b). Also, scanning electron microscopy was used to put in evidence the interface between HARDOX steel substrate and alumina coating as is shown in Fig. 5 (a, b).

These images highlight some surface aspects of the base material, and the thickness of the alumina layer deposited on the HARDOX steel. We can see that the deposited layer is homogeneous. Still, during the plasma jet deposition process, the powder reacts with the oxygen in the air during the deposition process. It forms a higher amount of oxides than those found in other thermal deposition processes. In some areas, we can observe small cracks between the deposited layers; these are formed during the cooling process due to internal stresses due to the thermal gradient.

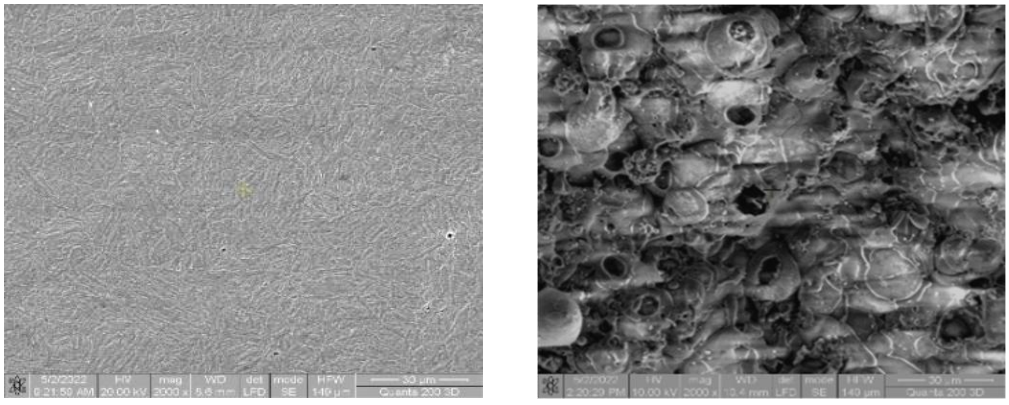

(a) (b)

Fig. 4. SEM images related to the sample surfaces: a) HARDOX steel 2000X, b) Alumina coatings on HARDOX steel 2000X

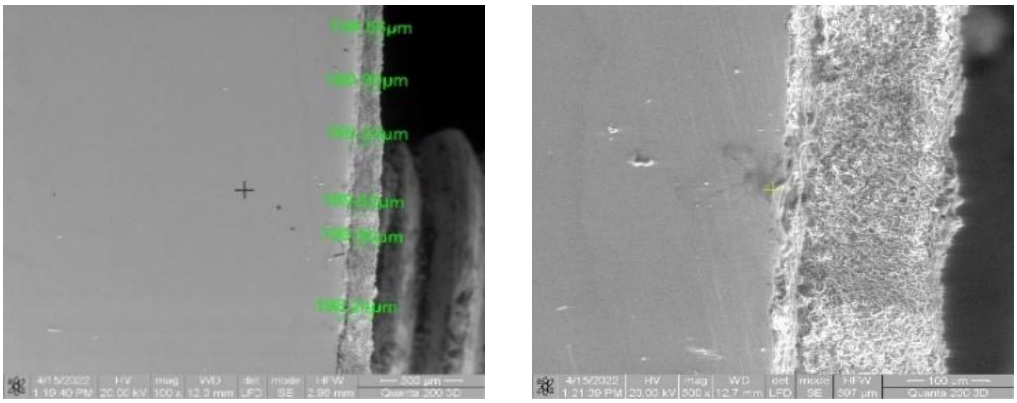

(a) (b)

Fig. 5. SEM images related to the interface between HARDOX steel substrate and alumina coatings: a) general view 100X, b) interface detail 500X

The deformation of the molten material particles upon impact with the substrate is highlighted. Adhesion to the layer interface presents a good qualitative aspect without unevenness. The layer's structure consists of columnar splats oriented in the direction of the thermal gradient formed during cooling.

3.3. XRD results

Following the XRD analyses conducted on both the base material and the coated material are presented in more detail in Fig. 6 (a, b), it was determined that the base material contained three compounds: $Fe_{1.00}Ni_{3.00}$, $Fe_{1.82}Si_{0.18}$, and $Fe_{4.00}$, all exhibiting a cubic structure.

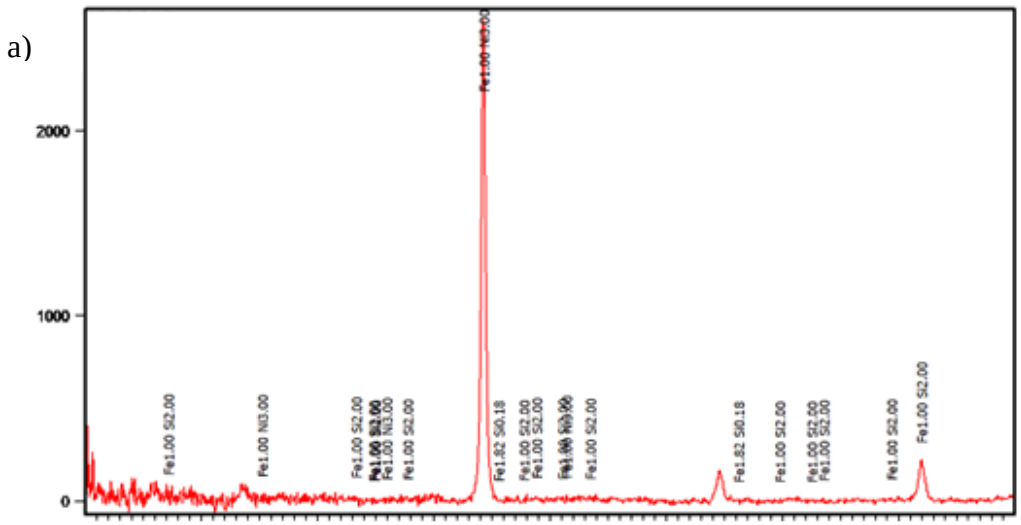

b)

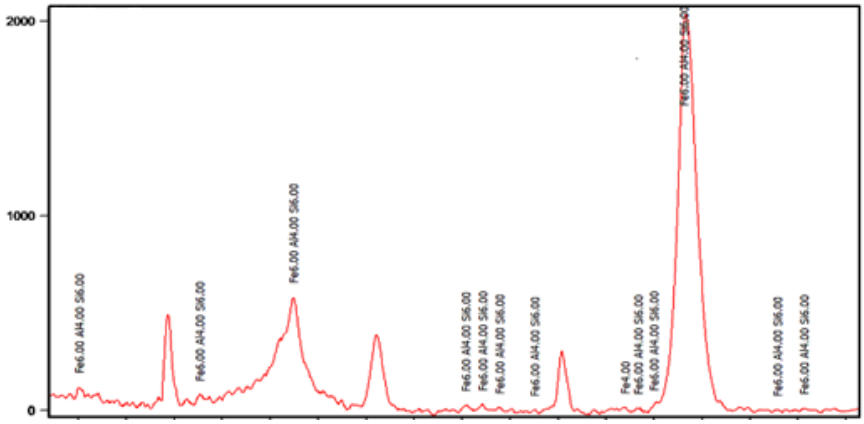

Fig. 6. XRD results: a) HARDOX steel, b) alumina coatings

In contrast, the coated material consists of two compounds: $Fe_{4.00}$, which has a cubic structure, and $Fe_{6.00}Al_{4.00}Si_{6.00}$, which possesses an anorthic structure. It was found that in the base material, the compound $Fe_{1.00}$ $Ni_{3.00}$ was highlighted at the angles 24.5°, 36.1°, 44°, and 53.4°, the compound $Fe_{1.82}$ $Si_{0.18}$ was highlighted at the angles 17.5°, 32.3°, 35.7°, 37° and 82°, and the compound $Fe_{4.00}$ stood out at the angles 45° and 78.2°.

3.4. Scratch and micro-indentation analysis

In the scratch tests, it was shown that the coefficient of friction (COF) is lower for the coated material than for the base material; for the base material, the COF is 0.883, and for the coated material, it is 0.651. A force of 10N was used for the micro indentation tests, and the results are in Table 2 and Fig. 7.

The micro indentation results show that the HARDOX steel has a higher modulus of elasticity than the alumina coating, respectively 110.93 GPa and 29.78 GPa. Also, the hardness is higher for the HARDOX steel than the alumina coating, respectively 2.16 GPa and 1.11 GPa.

Table 2

The results after the scratch and micro indentation tests			
HARDOX steel		**Alumina coating**	
Account. Stiffness (N/µm)	7.750	Account. Stiffness (N/µm)	3.111
Account. depth	3.351	Account. depth	6.564
Account. Area (µm^2)	4176.18	Account. Area (µm^2)	8113.586
Young's modulus (GPa)	110.936	Young's modulus (GPa)	29.78
Hardness (GPa)	2.16	Hardness (GPa)	1.11
Scratch test		*Scratch test*	
COF	0.883	COF	0.651

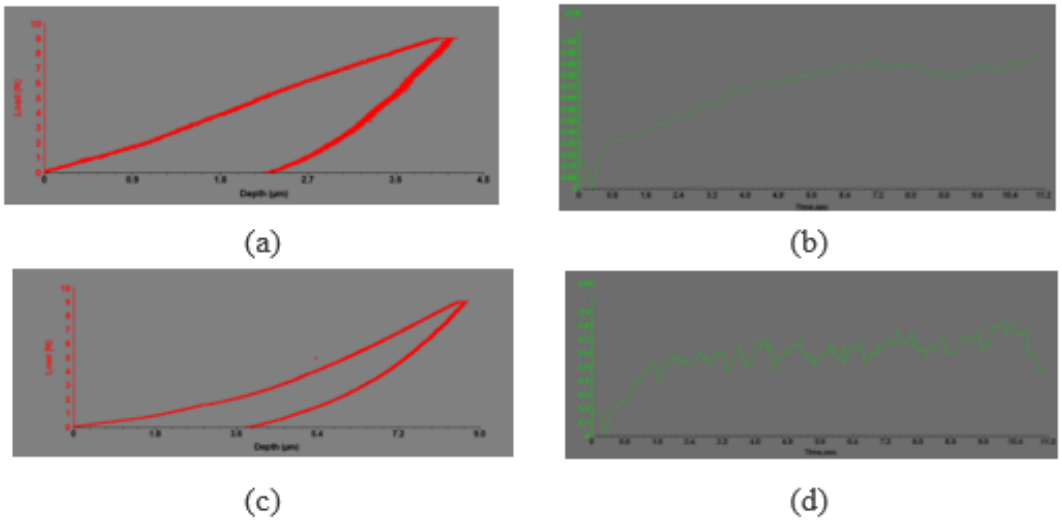

Fig. 7. The images recorded during the micro-indentation and micro-scratch test for the experimental samples: a) Micro indentation test for HARDOX steel, b) Scratch test for HARDOX steel, c) Micro indentation test for alumina coating, d) Scratch test for alumina coating

4. Conclusions

The structure after deposition is a layered columnar one, with lamellar and intralamellar cracks, large pores, and bridges between the neighboring slats. This structure is due to the deposition process because the particles of material with high kinetic energy hit the surface of the base material, and their kinetic energy is transformed into energy of variation of the shape of the particle, thus obtaining their elongated character. The high temperature of the particles leads to the appearance of internal stress due to their uneven contraction during the cooling process. This leads to the formation of microcracks at the interface of neighboring particles and inside them.

The micro indentation results show that the base material has a higher modulus of elasticity than the coated material, 110.93 GPa for the base material and 29.78 GPa for the coated material. Also, the hardness of the base material is higher than that of the coated material, 2.16 GPa for the base material and 1.11 GPa.

In conclusion, we could consider that alumina coatings on HARDOX steel are adherent and could be a solution for ballistic protection, but this fact must be demonstrated by future studies.

R E F E R E N C E S

1. Siengchin, S. A Review on Lightweight Materials for Defence Applications: Present and Future Developments. Defence Technology 2023, 24, 1–17, doi:10.1016/j.dt.2023.02.025.

2. Elveli, B.S.; Iddberg, M.B.; Børvik, T.; Aune, V. On the Strength–Ductility Trade-off in Thin Blast-Loaded Steel Plates with and without Initial Defects — An Experimental Study. Thin-Walled Structures 2022, 171, 108787, doi:10.1016/j.tws.2021.108787.
3. Krishnan, K.; Sockalingam, S.; Bansal, S.; Rajan, S.D. Numerical Simulation of Ceramic Composite Armor Subjected to Ballistic Impact. Composites Part B: Engineering 2010, 41, 583–593, doi:10.1016/j.compositesb.2010.10.001.
4. Jena, P.K.; Mishra, B.; RameshBabu, M.; Babu, A.; Singh, A.K.; SivaKumar, K.; Bhat, T.B. Effect of Heat Treatment on Mechanical and Ballistic Properties of a High Strength Armour Steel. International Journal of Impact Engineering 2010, 37, 242–249, doi:10.1016/j.ijimpeng.2009.09.003.
5. Baskutis, S.; Baskutiene, J.; Dragašius, E.; Kavaliauskiene, L.; Keršiene, N.; Kusyi, Y.; Stupnytskyy, V. Influence of Additives on the Mechanical Characteristics of Hardox 450 Steel Welds. Materials (Basel) 2023, 16, 5593, doi:10.3390/ma16165593.
6. Rubio-Ramirez, C.; Giarollo, D.F.; Mazzaferro, J.E.; Mazzaferro, C.P. Prediction of Angular Distortion Due GMAW Process of Thin-Sheets Hardox 450® Steel by Numerical Model and Artificial Neural Network. Journal of Manufacturing Processes 2021, 68, 1202–1213, doi:10.1016/j.jmapro.2021.06.045.
7. Kuntoglu, M. Machining Induced Tribological Investigations in Sustainable Milling of Hardox 500 Steel: A New Approach of Measurement Science. Measurement 2022, 201, 111715, doi:10.1016/j.measurement.2022.111715.
8. Moayyedian, M.; Mohajer, A.; Kazemian, M.G.; Mamedov, A.; Derakhshandeh, J.F. Surface Roughness Analysis in Milling Machining Using Design of Experiment. SN Appl. Sci. 2020, 2, 1698, doi:10.1007/s42452-020-03485-5.
9. Szymczak, T.; Kowalewski, Z.L. The High-Strength Steel and Its Weld under Impact. Materials Today: Proceedings 2022, 62, 2554–2559, doi:10.1016/j.matpr.2022.03.369.
10. Yılmaz, D.; Aktaş, B.; Çalık, A.; Aytar, O.B. Boronizing Effect on the Radiation Shielding Properties of Hardox 450 and Hardox HiTuf Steels. Radiation Physics and Chemistry 2019, 161, 55–59, doi:10.1016/j.radphyschem.2019.04.019.
11. Lasalvia, J.; Campbell, J.; Swab, J.; McCauley, J. Beyond Hardness: Ceramics and Ceramic-Based Composites for Protection. JOM 2010, 62, 16–23, doi:10.1007/s11837-010-0004-z.
12. Dresch, A.B.; Venturini, J.; Arcaro, S.; Montedo, O.R.K.; Bergmann, C.P. Ballistic Ceramics and Analysis of Their Mechanical Properties for Armour Applications: A Review. Ceramics International 2021, 47, 8743–8761, doi:10.1016/j.ceramint.2020.12.095.
13. Su, C.; Chen, B. Study on Effective Protective Area of Ceramic Composite Target. IOP Conf. Ser.: Mater. Sci. Eng. 2020, 768, 032013, doi:10.1088/1757-899X/768/3/032013.
14. Gonçalves, D.P.; de Melo, F.C.L.; Klein, A.N.; Al-Qureshi, H.A. Analysis and Investigation of Ballistic Impact on Ceramic/Metal Composite Armour. International Journal of Machine Tools and Manufacture 2004, 44, 307–316, doi:10.1016/j.ijmachtools.2003.09.005.
15. Fawaz, Z.; Zheng, W.; Behdinan, K. Numerical Simulation of Normal and Oblique Ballistic Impact on Ceramic Composite Armours. Composite Structures 2004, 63, 387–395, doi:10.1016/S0263-8223(03)00187-9.
16. Naik, N.; Kumar, S.; Ratnaveer, D.; Joshi, M.; Akella, K. An Energy-Based Model for Ballistic Impact Analysis of Ceramic-Composite Armors. International Journal of Damage Mechanics 2013, 22, 145–187, doi:10.1177/1056789511435346.
17. Konat, Ł. Technological, Microstructural and Strength Aspects of Welding and Post-Weld Heat Treatment of Martensitic, Wear-Resistant Hardox 600 Steel. Materials (Basel) 2021, 14, 4541, doi:10.3390/ma14164541.
18. Konat, Ł, Białobrzeska B., Białek P. Effect of Welding Process on Microstructural and Mechanical Characteristics of Hardox 600 Steel. Metals 2017, 7, 349, doi:10.3390/met7090349.

19. Konat, Ł.; Jasiński, R.; Białobrzeska, B.; Szczepański, Ł. Analysis of the Static and Dynamic Properties of Wear-Resistant Hardox 600 Steel in the Context of Its Application in Working Elements. Materials Science-Poland 2021, 39, 86–102.
20. Zhang, L.; Ji, C.; Wang, X.; Wang, Y.; Wu, G.; Zhu, H.; Han, Z. Strengthening and Converse Strengthening Effects of Polyurea Layer on Polyurea–Steel Composite Structure Subjected to Combined Actions of Blast and Fragments. Thin-Walled Structures 2022, 178, 109527, doi:10.1016/j.tws.2022.109527.
21. Toutanji, H.A.; Choi, H.; Wong, D.; Gilbert, J.A.; Alldredge, D.J. Applying a Polyurea Coating to High-Performance Organic Cementitious Materials. Construction and Building Materials 2013, 38, 1170–1179, doi:10.1016/j.conbuildmat.2012.09.041.
22. Mariappan, S.; Radhika, N.; Saleh, B. Duplex and Composite Coatings: A Thematic Review on Thermal Spray Techniques and Applications. Metals and Materials International 2022, 29, doi:10.1007/s12540-022-01302-9.
23. Dorfman, M. Thermal Spray Coatings. Handbook of Environmental Degradation of Materials 2005, 405–422, doi:10.1016/B978-081551500-5.50022-7.
24. Herman, H.; Sampath, S.; McCune, R. Thermal Spray: Current Status and Future Trends. MRS Bulletin 2000, 25, 17–25, doi:10.1557/mrs2000.119.
25. Jiang, X.-Y.; Hu, J.; Jiang, S.-L.; Wang, X.; Zhang, L.-B.; Li, Q.; Lu, H.-P.; Yin, L.-J.; Xie, J.-L.; Deng, L.-J. Effect of High-Enthalpy Atmospheric Plasma Spraying Parameters on the Mechanical and Wear Resistant Properties of Alumina Ceramic Coatings. Surface and Coatings Technology 2021, 418, 127193, doi:10.1016/j.surfcoat.2021.127193.
26. Szkodo, M.; Bień, A.; Antoszkiewicz, M. Effect of Plasma Sprayed and Laser Re-Melted Al_2O_3 Coatings on Hardness and Wear Properties of Stainless Steel. Ceramics International 2016, 42, 11275–11284, doi:10.1016/j.ceramint.2016.04.044.
27. Bejinariu, C.; Paleu, V.; Stamate, C.; Cimpoesu, R.; Coteata, M.; Bădărău, G.; Axinte, M.; Istrate, B.; Vasilescu, G.; Cimpoesu, N. Microstructural, Corrosion Resistance, and Tribological Properties of Al2O3 Coatings Prepared by Atmospheric Plasma Spraying. Materials 2022, 15, doi:10.3390/ma15249013.
28. Maruszczyk, A.; Dudek, A.; Szala, M. Research into Morphology and Properties of TiO_2 – NiAl Atmospheric Plasma Sprayed Coating. Advances in Science and Technology Research Journal 2017, 11, 204.
29. Wang, M.; Shaw, L.L. Effects of the Powder Manufacturing Method on Microstructure and Wear Performance of Plasma Sprayed Alumina–Titania Coatings. Surface and Coatings Technology 2007, 202, 34–44, doi:10.1016/j.surfcoat.2007.04.057.
30. Aruna, S.T.; Balaji, N.; Shedthi, J.; Grips, V.K.W. Effect of Critical Plasma Spray Parameters on the Microstructure, Microhardness and Wear and Corrosion Resistance of Plasma Sprayed Alumina Coatings. Surface and Coatings Technology 2012, 208, 92–100, doi:10.1016/j.surfcoat.2012.08.016.
31. Spyra, J.; Michalak, M.; Niemiec, A.; Łatka, L. Mechanical Properties Investigations of the Plasma Sprayed Coatings Based on Alumina Powder. Welding Technology Review 2020, 92, 17–23, doi:10.26628/wtr.v92i4.1107.